(In,Ga)N/GaN microcavities with double dielectric mirrors fabricated by selective removal of an (Al,In)N sacrificial layer

F. Rizzi[a)]
Institute of Photonics, SUPA, University of Strathclyde, 106 Rottenrow, Glasgow G4 0NW, United Kingdom

P. R. Edwards and K. Bejtka[b)]
Department of Physics, SUPA, University of Strathclyde, 107 Rottenrow, Glasgow G4 0NG, United Kingdom

F. Semond
CRHEA-CNRS, Rue Bernard Gregory, Parc Sophia Antipolis, 06560 Valbonne, France

X. N. Kang and G. Y. Zhang
Research Center for Wide-Gap Semiconductors, State Key Laboratory for Mesoscopic Physics, Peking University, Beijing 100871, People's Republic of China

E. Gu, M. D. Dawson, and I. M. Watson
Institute of Photonics, SUPA, University of Strathclyde, 106 Rottenrow, Glasgow G4 0NW, United Kingdom

R. W. Martin[c)]
Department of Physics, SUPA, University of Strathclyde, 107 Rottenrow, Glasgow G4 0NG, United Kingdom

(Received 29 November 2006; accepted 5 February 2007; published online 15 March 2007)

Comparable microcavities with $3\lambda/2$ (~240 nm) active regions containing distributed (In,Ga)N quantum wells, grown on GaN substrates and bounded by two dielectric mirrors, have been fabricated by two different routes: one using laser lift-off to process structures grown on GaN-on-sapphire templates and the second using freestanding GaN substrates, which are initially processed by mechanical thinning. Both exploit the properties of an $Al_{0.83}In_{0.17}N$ layer, lattice matched to the GaN substrate and spacer layers. In both cases cavity quality factors >400 are demonstrated by measurements of the cavity-filtered room-temperature excitonic emission near 410 nm. © *2007 American Institute of Physics*. [DOI: 10.1063/1.2712786]

Applications of III-nitride-based semiconductors continue to expand and diversify. Commercialized devices include UV blue-green light-emitting diodes, edge-emitting blue laser diodes, and transistors.[1] Future devices will include vertical cavity surface emitting lasers and related structures. In particular, the high exciton binding energies and oscillator strengths for bulk GaN and III-nitride heterostructures make microcavity (MC) structures very promising for room-temperature operation of devices such as polariton lasers or optical amplifiers.[2] GaN-based MCs have been fabricated using a variety of processing routes. Recently, good progress has been made on fully epitaxial MCs, in which both distributed Bragg reflectors (DBRs) comprise III-nitride multilayers.[3,4] However, growth of such MCs requires lengthy and demanding growth processes to combat strain and cracking issues, and the resulting III-nitride DBRs still have relatively narrow high-reflectivity stop bands. In other cases, a so-called hybrid approach was used, combining one epitaxial semiconductor mirror with a second metallic or dielectric mirror.[5,6] The so-called fully hybrid approach exploits the well-established properties of high-reflectivity dielectric DBRs for both upper and lower mirrors, and offers the potential for higher finesse MCs.[7–10] Fabricating a MC of this type requires accessing the underside of the active region by removal of the substrate and buffer layers. Laser lift-off (LLO) from a sapphire substrate,[7,8] plasma etching of a SiC substrate,[9] and wet chemical etching of a silicon substrate[10] have all been employed to achieve this. After substrate removal, further thinning of buffer layers is usually required to accurately define the desired cavity length, and it is essential to have a reliable method to achieve this objective.

In this letter, we describe the properties of two types of fully hybrid III-nitride MCs fabricated using a sacrificial $Al_{0.83}In_{0.17}N$ layer to perform key roles in the growth and fabrication sequence. Both processing routes utilize recently available substrates with low threading dislocation densities and consequent benefits for the structural quality of the MC active region. One approach uses 10×10 mm^2 freestanding GaN (FS-GaN) substrates, and here postgrowth processing begins with mechanical grinding of the substrate back side. Larger FS-GaN substrates have since become more readily available and are expected to give better results due to reduced edge effects. The other approach employs 2 inch GaN-on-sapphire templates, using LLO to remove the substrate from 6×6 mm^2 squares in a single rapid step. In both cases, an $Al_{0.83}In_{0.17}N$ layer is included in the epitaxial structure immediately below an (In,Ga)N/GaN MC active region. This ultimately acts as a sacrificial layer in a selective wet etching step,[11] but also allows endpoint detection during plasma etch steps which precede this. The sacrificial $Al_{0.83}In_{0.17}N$ is lattice matched to GaN,[3,12] and the high quality of GaN grown above such a layer has recently been confirmed by spectroscopic and structural characterization.[13] The refractive index contrast between $Al_{0.83}In_{0.17}N$ and GaN is also valuable in facilitating *in situ* reflectometry during epitaxy on FS-GaN.[14,15]

[a)]Also at: Department of Physics, University of Strathclyde, Glasgow, UK.
[b)]Also at: Institute of Photonics, University of Strathclyde, Glasgow, UK.
[c)]Electronic mail: r.w.martin@strath.ac.uk

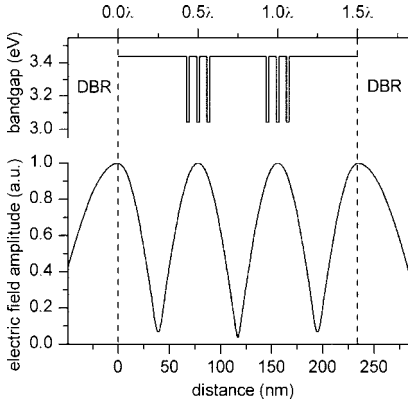

FIG. 1. Schematic representation of the band gap variation and calculated electric field distribution in the (In,Ga)N/GaN MC active region.

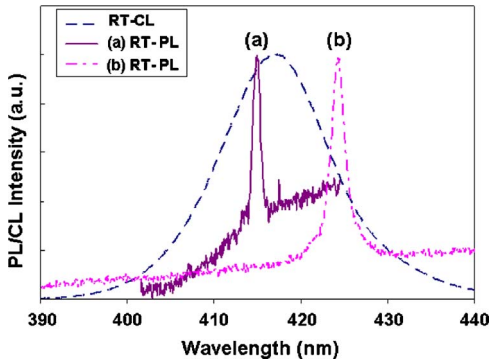

FIG. 2. (Color online) RT-PL spectra from the MC grown on FS-GaN, plotted as continuous lines. Spectra (a) and (b) correspond to different areas. A RT-CL spectrum from the back side of the active region before deposition of the second DBR is plotted as a dashed line.

Growth of the nitride heterostructures used an Aixtron 200 series metal-organic vapor phase epitaxy (MOVPE) reactor, fitted with a multiwavelength, normal-incidence reflectometer. FS-GaN and ultralow defect (ULD) GaN-on-sapphire templates were supplied by Lumilog (Vallauris, France). Both had (0001) orientation with a Ga-polar top surface. The FS-GaN substrates were approximately 300 μm in thickness, while the ULD-GaN templates consisted of 8–10 μm layers of GaN grown by MOVPE, using proprietary dislocation filtering techniques. More details on growth conditions and the substrates are reported elsewhere.[13–15] Growth of each MC structure began with a GaN buffer layer, followed by the $Al_{0.83}In_{0.17}N$ sacrificial layer with a nominal thickness of 70 nm, chosen to give a readily interpretable *in situ* reflectance waveform at a monitoring wavelength of 625 nm.[15] The MC active region was grown directly above the $Al_{0.83}In_{0.17}N$ layer and contained two groups of three $\approx$2.5 nm thick $In_{0.08}Ga_{0.92}N$ quantum wells (QWs), positioned symmetrically within the MC at electric field antinode positions, as illustrated in Fig. 1. The optical thickness of $3\lambda/2$ corresponds to a total physical thickness of $\sim$240 nm. Both DBRs comprised ten repeat periods of SiO_2/ZrO_2 quarter-wavelength layers deposited by electron beam evaporation, with an optimum reflectivity of 99.7% and a center wavelength at 410 nm, closely matched to the measured QW peak emission wavelength. The first of the DBRs was deposited on top of the active MC layers following the epitaxial growth. The second was deposited on the lower MC surface following the processing steps described below.

After deposition of the top mirror, the top surface of this DBR was bonded to a sapphire carrier using UV-curable optical cement. As a result N-face GaN $(000\bar{1})$ faces away from the carrier and will be subsequently processed. The process flow now followed one of two routes, depending on which substrate type had been used in the growth. A summary is provided here, but more details on several steps, particularly optimization of plasma etching for N-polar GaN, is reported elsewhere.[16] For MCs on FS-GaN, mechanical grinding was employed as a fast method to reduce the substrate thickness to a few tens of microns. A chemomechanical polishing step was used to recover a smooth surface after grinding. For the MCs on ULD-GaN templates, the first step involved LLO using a KrF excimer laser to remove the epitaxial layers from the sapphire substrate. Next, in both variants of the process flow, the remaining few tens of microns of GaN above the $Al_{0.83}In_{0.17}N$ were removed, stopping within the ternary layer. This was achieved by plasma etching employing a reflectivity-based endpoint detection technique.[17] Having stopped the plasma etch just after penetration into the sacrificial layer, the remaining $Al_{0.83}In_{0.17}N$ was removed using selective wet etching an aqueous solution of a chelating amine MC.[11,17] Ideally this process will stop cleanly at the epitaxial interface between $Al_{0.83}In_{0.17}N$ and GaN, removing any requirement for the plasma etching steps themselves to leave an optically smooth surface. Thus the scale of surface roughness must only be limited to values below the $Al_{0.83}In_{0.17}N$ thickness. Finally, a second dielectric DBR, of similar specification to the first, was deposited on the N-face GaN surface of the active region.

The optical properties of the MCs were analyzed using photoluminescence (PL) and cathodoluminescence (CL) spectra. CL spectra were collected in the surface-normal direction from "half-cavities," prior to deposition of the second DBR, using an electron probe microanalyzer and a defocused electron beam ($\approx$10 μm diameter).[18] The optical properties of the completed MCs were assessed by PL excited with either a 325 nm HeCd or a 244 nm frequency-doubled Ar^+ laser. The laser was focused by eye using only a singlet lens, giving a spot size in the region of 50 μm. Both PL excitation and collection were performed through the N-face mirror, with a laser incidence angle of 30°–40° from the normal for the He-Cd laser and almost normal for the doubled Ar^+ laser. The emitted light was collected in the surface-normal direction in all cases, apart from the angle-resolved measurements mentioned below.

Figures 2 and 3 show typical luminescence spectra, each

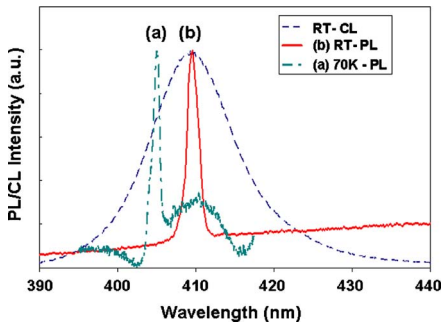

FIG. 3. (Color online) PL and CL spectra from the MC grown on an ULD-GaN template. PL were acquired with (a) a doubled Ar^+ laser at 70 K and (b) a HeCd laser at RT from different areas. The dashed line shows the RT-CL spectrum from the back side of the active region before deposition of the second DBR.

comparing CL from a half-cavity structure with PL emission from completed MCs. Figure 2 shows results from a MC grown on FS-GaN, while Fig. 3 shows results from a structure grown on ULD-GaN. The room-temperature (RT) CL spectra show the expected excitonic luminescence peak from the QWs, with maxima at wavelengths of 417 and 409 nm, respectively, for the two samples. The full widths at half maximum (FWHMs) are 111 and 95 meV. These reflect the conventional narrowing of the QW luminescence as the peak wavelength decreases. Single QWs from our reactor, with peak emission wavelengths at 390 nm, show low-temperature FWHM down to 45 meV. After completion of the MCs by deposition of the second mirror, the luminescence is strongly filtered by the cavity mode, and considerably sharper peaks were observed. Figure 2 shows two RT-PL spectra from the completed MC, representative of measurements across several mm^2 of the sample. One peak, labeled (a), has a FWHM of 1.0 nm (7 meV) and is centered on a wavelength of 415 nm. This corresponds to a cavity quality factor ($Q=\lambda/\Delta\lambda$) of 415. A different region of the sample gives a shifted peak centered at 424 nm, labeled (b), with a slightly broader FWHM (1.9 nm). Characterization of the LLO-processed sample included low-temperature PL measurements at 70 K, using 244 nm excitation. The resulting spectra showed a sharper cavity mode peak, centered on a wavelength of 405 nm, and superimposed on an excitonic peak very similar to that observed in the CL from the half-cavity [Fig. 3(a)]. The FWHM of 0.7 nm (5 meV) gives a cavity Q factor of 580. Figure 3(b) shows a typical RT-PL spectrum obtained with HeCd excitation, giving a broader cavity-filtered PL peak at slightly longer wavelength. Angle-resolved PL measurements, in which the detection was angled at up to 32°, show a conventional dispersion of this cavity mode. In this case the excitonic mode is too broad and at too low an energy to see polariton coupling effects.[5,6,9] The measured Q factors lie within the range of the best reported values (400–750) for similar MCs with double dielectric Bragg mirrors[7–9] but here the use of GaN substrates with low threading dislocation densities gives the added benefit of improved epitaxial quality.

As will be apparent from the examples discussed, measurements at different points on the two MCs produced significantly different PL spectra. Transfer matrix simulations indicate that fluctuations in the active region thicknesses of ~12 nm for the sample grown on FS-GaN and ~5 nm for the sample grown on ULD-GaN are sufficient to account for the shift of the cavity mode. Such fluctuations are likely to result from issues in control of the final etch-based fabrication steps at their current stage of development. Figure 4 shows a cross-sectional scanning electron microscope image of the MC fabricated on FS-GaN, taken following the optical measurements. Undulations on a scale consistent with the apparent MC thickness variations from simulations are evident in the upper DBR, reflecting surface roughness resulting from the processing. Optimization of the etching of the AlInN sacrificial layer is under way to reduce this.

In summary, we have demonstrated two processing routes for epitaxial GaN-based MCs with double dielectric Bragg mirrors. An $Al_{0.83}In_{0.17}N$ sacrificial layer, lattice matched to GaN, is used to facilitate controlled removal of material from under the active region. Postgrowth processing began with mechanical grinding for structures grown on

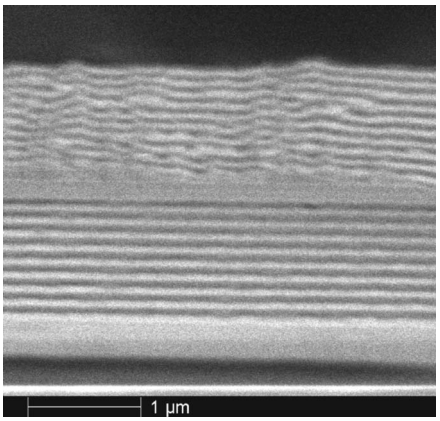

FIG. 4. Cross-sectional scanning electron microscopy image of the microcavity on FS-GaN.

freestanding GaN or laser lift-off in the case of those grown on GaN-on-sapphire templates. Cavity-filtered excitonic PL peaks were observed in both cases, giving Q factors in the range of 400–600. These approaches open the way to improved structural quality of the active region, resulting from the use of substrates with low threading dislocation densities.

The authors thank S. Christopolous and J. J. Baumberg (Southampton University, UK) for providing the angle-resolved PL data and acknowledge funding from the EU projects CLERMONT2 (MRTN-CT-2003-503577) and STIMSCAT (STREP Contract No. 517769).

[1] S. Nakamura, G. Fasol, and S. J. Pearton, *The Blue Laser Diode: The Complete Story* (Springer, New York, 2000).
[2] G. Malpuech, A. Di Carlo, A. V. Kavokin, J. J. Baumberg, A. Zamfirescu, and P. Lugli, Appl. Phys. Lett. **81**, 412 (2002).
[3] J.-F. Carlin, J. Dorsaz, E. Feltin, R. Butté, N. Grandjean, M. Ilegems, and M. Läugt, Appl. Phys. Lett. **86**, 031107 (2005).
[4] X. H. Zhang, S. J. Chua, W. Liu, L. S. Wang, A. M. Yong, and S. Y. Chow, Appl. Phys. Lett. **88**, 191111 (2006).
[5] F. Semond, I. R. Sellers, F. Natali, D. Byrne, M. Leroux, J. Massies, N. Ollier, J. Leymarie, P. Disseix, and A. Vasson, Appl. Phys. Lett. **87**, 021102 (2005).
[6] E. Feltin, G. Christmann, R. Butté, J.-F. Carlin, M. Mosca, and N. Grandjean, Appl. Phys. Lett. **89**, 071107 (2006).
[7] Y.-K. Song, H. Zhou, M. Diagne, I. Ozden, A. Vertikov, A. V. Nurmikko, C. Carter-Coman, R. S. Kern, F. A. Kish, and M. R. Krames, Appl. Phys. Lett. **74**, 3441 (1999).
[8] R. W. Martin, P. R. Edwards, H.-S. Kim, K.-S. Kim, T. Kim, I. M. Watson, M. D. Dawson, Y. Cho, T. Sands, and N. W. Cheung, Appl. Phys. Lett. **79**, 3029 (2001).
[9] T. Tawara, H. Gotoh, T. Akasaka, N. Kobayashi, and T. Saitoh, Phys. Rev. Lett. **92**, 256402 (2004).
[10] T. K. Kim, S. S. Yang, J. K. Hong, and G. M. Yang, Appl. Phys. Lett. **89**, 041129 (2006).
[11] F. Rizzi, K. Bejtka, P. R. Edwards, R. W. Martin, and I. M. Watson, J. Cryst. Growth **300**, 254 (2007).
[12] K. Lorenz, N. Franco, E. Alves, I. M. Watson, R. W. Martin, and K. P. O'Donnell, Phys. Rev. Lett. **97**, 085501 (2006).
[13] K. Bejtka, R. W. Martin, I. M. Watson, S. Ndiaye, and M. Leroux, Appl. Phys. Lett. **89**, 191912 (2006).
[14] I. M. Watson, C. Liu, E. Gu, M. D. Dawson, P. R. Edwards, and R. W. Martin, Appl. Phys. Lett. **87**, 151901 (2005).
[15] K. Bejtka, F. Rizzi, P. R. Edwards, R. W. Martin, E. Gu, M. D. Dawson, I. M. Watson, I. R. Sellers, and F. Semond, Phys. Status Solidi A **202**, 2648 (2005).
[16] F. Rizzi, E. Gu, M. D. Dawson, I. M. Watson, R. W. Martin, X. N. Kang, and G. Y. Zhang, J. Vac. Sci. Technol. A **25**, 252 (2007).
[17] F. Rizzi, P. R. Edwards, I. M. Watson, and R. W. Martin, Superlattices Microstruct. **40**, 369 (2006).
[18] R. W. Martin, P. R. Edwards, K. P. O'Donnell, M. D. Dawson, C.-W. Jeon, C. Liu, G. R. Rice, and I. M. Watson, Phys. Status Solidi A **201**, 665 (2004).